Two-dimensional exchange ^{2}H NMR experiments of phospholipid bilayers on a spherical solid support

C. Dolainsky,[1] M. Unger,[1] M. Bloom,[2] and T. M. Bayerl[3]
[1]*Physik Department E22, Technische Universität München, D-85747 Garching, Germany*
[2]*Department of Physics, University of British Columbia, Vancouver, Canada V6T 1Z1*
[3]*Physikalisches Institut EP-V, Universität Würzburg, 97047 Würzburg, Germany*
(Received 12 October 1994)

Bilayers of 1-palmitoyl-2-oleoyl-*sn*-glycero-3-phosphocholine (POPC) on a spherical solid support consisting of silica beads are studied by two-dimensional exchange deuterium NMR (2D exchange ^{2}H NMR) at two hydration states of the bilayer and at mixing times in the range 1–8 ms. The spectra obtained were analyzed in terms of a solution of the diffusion equation of molecules diffusing on the surface of a sphere with a radius corresponding to that of the solid support. This procedure gives a jump angle distribution function of the lipids for a fixed mixing time. The well defined geometry of the sample enables us to compare the experimental results with those obtained by a random walk simulation assuming that solely diffusional jumps of the POPC molecules contribute to the 2D exchange NMR spectra during the mixing time. Excellent agreement was obtained between the experimental results, computer simulations, and numerical calculations based on the diffusion equation. These results provide strong evidence that lateral diffusion of lipids is the dominant mechanism in determining the spectral evolution in 2D exchange NMR spectroscopy of spherical, solid supported lipid bilayers. From the experiments we obtained a lateral diffusion coefficient of the POPC molecules of $D=(8.2\pm3)\times10^{-12}$ m^2/s (high hydration, $T=30$ °C) and of $D=(0.8\pm0.4)\times10^{-12}$ m^2/s (low hydration, $T=35$ °C) in good agreement with values obtained previously using other spectroscopic methods. From these results it is concluded that future applications of the 2D exchange NMR method may provide valuable insight into the shapes and the slow motion dynamics of biological membranes.

PACS number(s): 61.30.-v, 76.60.−k, 87.22.−q

I. INTRODUCTION

Nuclear magnetic resonance (NMR) occupies a special niche in the hierarchy of spectroscopic techniques. Its natural time scale is longer than that of other spectroscopic techniques, corresponding to $\tau_{\rm NMR}\geq10^{-5}$ s for typical nuclear spins such as protons (^{1}H), deuterons (^{2}H), phosphorus (^{31}P), and carbon (^{13}C) that have proven to be useful in the study of fluid lipid bilayer membranes. The spectral characteristics represent averages over fast fluctuations of the spin-dependent interactions having correlation times $\tau_c\ll\tau_{\rm NMR}$, while the transverse relaxation time T_2 is sensitive to slower motions, i.e., those with $\tau_c\approx\tau_{\rm NMR}$ [1–4]. A powerful NMR technique for studying in a precise manner very slow motions, i.e, those having correlation times $\tau_c\gg\tau_{\rm NMR}$, was developed recently by Spiess and his co-workers [5–8]. In this so called two-dimensional (2D) exchange ^{2}H NMR, the phases of the spins are initially labeled by their spectral frequency ω_1, the molecular position and internal coordinates are allowed to evolve for a "mixing time" t_m, and the spectral frequency ω_2 is then recorded. For the case of fluid lipid bilayers ω_1 and ω_2 are related to the angles θ_1 and θ_2 between the surface normal and the external magnetic field by

$$\omega_i=\omega_q S_{\rm CD}P_2(\cos\theta_i)=\omega_q S_{\rm CD}(3\cos^2\theta_i-1)/2\ , \quad (1)$$

where ω_q is the quadrupolar coupling frequency and $S_{\rm CD}$ is the orientational order parameter for the C═D bond. The two dimensional spectrum $S(\omega_1,\omega_2;t_m)$ so defined then gives the joint probability that a given spin has spectral frequencies ω_1 and ω_2 at times separated by t_m. This technique has great potential in the study of fluid membranes. There the molecules typically diffuse a distance $L_{\rm NMR}\approx(4D\tau_{\rm NMR})^{1/2}$ on the order of several hundred angstroms during a time $\tau_{\rm NMR}$. Information about physical phenomena associated with such mesoscopic distances has been particularly elusive up to now. The applicability of 2D exchange NMR to fluid and gel state membranes has been demonstrated by Auger and coworkers [9,10] using ^{2}H NMR and by Fenske and coworkers [11,12] using ^{31}P NMR.

The geometry of biological membranes is very complex and even the widely used multilamellar dispersions of lipid bilayer model membranes are usually not well defined. Since the ^{2}H NMR spectral frequency is dependent on the orientation of the local bilayer normal as well as on the local bilayer thickness [13], several different physical mechanisms may be associated with $S(\omega_1,\omega_2;t_m)$. Indeed the study of 2D exchange ^{2}H NMR in a fluid multilamellar dispersion reported in the accompanying (preceding) paper [14] shows some interesting complexity. The purpose of the work reported here is to isolate one of the important mechanisms contributing to $S(\omega_1\omega_2;t_m)$ in a particularly simple model system and to check on whether our basic ideas on this mechanism are quantitatively correct.

The mechanism we shall explore is associated with diffusion of molecules on curved surfaces. From Eq. (1), we see that, if S_{CD} does not change appreciably for $t_m > \tau_{NMR}$, measurement of $S(\omega_1,\omega_2;t_m)$ can in principle yield the joint probability $P(\theta_1,\theta_2;t_m)$ that the local surface normal is oriented at θ_1 initially and θ_2 after the time t_m. The model system studied consists of a well defined number of bilayers on a solid spherical support of known diameter. From previous work on this system [15] we believe that our spherical solid supported lipid bilayers have the property that both the local bilayer thickness and the curvature fluctuations are not dominant [4,16] so that $P(\theta_1,\theta_2;t_m)$ can be adequately represented as a solution of the diffusion equation on a sphere of radius $R \gg L_{NMR}$. In such case the probability that after the mixing time the local surface normal for a given molecule will have changed by an angle β is given by

$$P(\beta,t_m)=\tfrac{1}{2}\sum_{l=0}^{\infty}(2l+1)P_l(\cos\beta)e^{-t_m/\tau_1}\sin\beta\ , \tag{2}$$

with

$$1/\tau_1 = l(l+1)D/R^2\ , \tag{3}$$

where D is the diffusion constant of the molecule on the spherical surface and P_l is a Legendre polynomial of order l. Analysis of the 2D ^{2}H NMR data using methods described in the preceding paper and in Sec. III yields $P^*(\beta;t_m)$

$$P^*(\beta,t_m)=\tfrac{1}{2}[P(\beta,t_m)+P(\pi-\beta,t_m)]\ . \tag{4}$$

The set of computations required to go from the experimental 2D NMR spectrum to the determination of the experimental $P^*(\beta;t_m)$ to be compared with Eq. (4) is quite complicated even for the simple case that only diffusion contributes to $S(\omega_1,\omega_2;t_m)$. For this reason, after describing the materials and methods in our experiments we devote Sec. III to a comparison of the analysis of $P^*(\beta;t_m)$ obtained from simulated 2D spectra with a diffusive motion on a sphere, simulated via discrete jumps, with the theoretical form of Eq. (2). This is followed by a report of results obtained for a fully hydrated spherical supported multibilayer sample using two different mixing times and of a study of a sample having significantly lower hydration and, hence, a lower value of the diffusion constant. Finally, we discuss the implications of our results in relation to those reported in the accompanying paper and future work, using the 2D exchange NMR method.

II. MATERIALS AND METHODS

1-palmitoyl-(6,6)-D_2-2-oleoyl-phosphocholine (POPC-6-d_2) was synthesized by Ruthven N. A. H. Lewis (Dept. of Biochemistry, University of Alberta, Edmonton, Canada). It is deuterated on the sixth carbon of the palmitic acid chain. Silica beads were obtained from Degussa (Hanau, German) with a radius of 320±20 nm.

The experiments were performed on a home-built spectrometer at the Physics Department of the University of British Columbia (Vancouver, Canada) [17] at a ^{2}H NMR resonance frequency of 46 MHz. A home-built probe with a 10 mm coil and a $\pi/2$ pulse length of 4 μs was used. 23 000 scans were acquired with a recycle delay of 200 ms. Constant temperatures were maintained using a Bruker model BV-T1000 temperature controller.

2D exchange spectra were recorded with a pulse sequence presented by Schmidt, Blümich, and Spiess [5]: 90_y-t_1-54.7_ϕ-t_m-54.7_ϕ-Δ-90_x-Δ-t_2. Quadrature detection in t_1 was achieved using a similar phase cycling scheme for the phase ϕ as described by Schmidt *et al.* Phase cycling was extended to account for imperfections of the last pulse, according to the 8-CYCLOPS phase cycle [18] for a quadrupolar echo. Spectra for mixing times of 2 and 4 ms were recorded with 128 different t_1 values. The lowest t_1 value was 0.3 μs. 256 complex values were acquired with quadrature detection in t_2. The dwell time was 5 μs in both dimensions and a refocusing time Δ of 40 μs was used.

The time domain data were shifted back to $t_1=0$ using a third order polynomial interpolation. They were Fourier transformed from the top of the echo in t_2 at Δμs after the last pulse after shifted sine bell and Lorentzian apodization in both dimensions and zero filling in t_1 to 256 points. The procedure described by Schmidt, Blümich, and Spiess [5] was followed to obtain a pure absorption mode 2D powder spectrum. A zero order baseline correction was applied to the spectra.

The solid supported multilayer vesicles (SSMV) were prepared as described in Ref. [4]. A 50 mg/ml solution of 120 mg POPC-6-d_2 was sonicated to give small unilamellar vesicles. This solution was dried together with the amount of silica beads (0.6 g) required to form approximately 20 lipid bilayers. After annealing at 60 °C for 4 h the samples were rehydrated using ^{2}H-depleted water. Two hydrations were adjusted for $r=320$ nm SSMV's: Full hydration (19–20 wt. % [19,20]) was achieved by rehydrating under water vapor atmosphere without any salt. For a low hydration (6–8 wt %) a petri dish with LiCl was added to the desiccator. The temperature of the liquid crystalline phase transition was determined before and after the 2D experiments from the ^{2}H NMR line shape. It was below 5 °C in the first case and at 30 °C for the low hydration samples. The experiments were performed at 30 °C with the fully hydrated and at 35 °C with the low hydration sample.

III. SIMULATIONS AND DATA ANALYSIS

A. Theoretical probability distributions for diffusion on a sphere

To calculate the probability distribution $P(\beta)$ for a jump over an angle β during the mixing time a discrete version of the diffusion equation in spherical symmetry is solved as described in the work of Wefing, Kaufmann, and Spiess [7]. One gets then an expression for the two-time distribution $P(\theta_1,\theta_2;t_m)$, where θ_1 denotes the orientation of the local surface normal during the evolution time and θ_2 during the acquisition period. This discrete approximation was used instead of the solution expressed as a series of Legendre polynomials [Eq. (2)]. Thus the

problem is reduced to solving an eigenvalue problem of a tridiagonal matrix. Jumps between 60 discrete sites were considered, giving a resolution of 3° in the jump angle. The reorientation angle distribution(RAD) $P(\beta)$ is then given by the two-time probability $P(\theta_1=0,\theta_2=\beta;t_m)$, which takes the form of Eq. (2) for the continuous limit.

B. Calculation of jump angle distributions from 2D exchange spectra

The procedure used is similar to that described in the preceding paper [14]. The kernel functions $K_{\|}(t_1,t_2|\beta)$ $(1\in\{\cos,\sin\})$, giving the 2D exchange time-domain signals for a discrete jump over an angle β during the mixing time, were calculated using the theoretical line shapes for a powder sample given by Grabowski and Hohnerkamp [21]. A numerical integration was used to solve the integrals for the time-domain data. For the fully hydrated POPC-6-d_2 sample a quadrupolar splitting of 30.2 kHz was obtained from fitting a powder line shape to a spectrum acquired by a quadrupolar echo. The line shape analysis was done first with a frequency-independent exponential T_2 relaxation with a time constant of 280 μs. To increase the quality of the line shape fit, a frequency-dependent T_2 relaxation time as obtained from experimental data was taken into account. For the low hydration sample we found a splitting of 38.4 kHz and a relaxation time of 280 μs. We chose a resolution of 3° in β and thus had to calculate a set of 30 theoretical kernel functions $K_{\|}(t_1,t_2|\beta)$ for the different discrete jump angles β. Dwell times and number of t_1 steps were the same as in experimental data sets. The theoretical spectra $S_{\text{theor}}(\omega_1,\omega_2|\beta)$ were then obtained from the time-domain data $K_{\|}(t_1,t_2|\beta)$ using the same procedure as for the experimental spectra.

As can be seen from Eq. (1), one cannot distinguish between jumps of β and π-β in ^{2}H NMR. Thus the resulting experimental reorientation angle distribution $P^*(\beta)$ is a sum of the underlying jump angle distributions $P(\beta)$ and $P(\pi-\beta)$ [cf. Eq. (4)].

To get the experimental RAD $P^*(\beta)$, the experimental spectra are seen as a superposition of submatrices $S_{\text{theor}}(\omega_1,\omega_2|\beta)$. A minimization procedure was programmed to find the statistical weight $P^*(\beta)$ of the submatrix $S_{\text{theor}}(\omega_1,\omega_2|\beta)$ by minimizing the quadratic form $\mathbf{R}(P^*(\beta))$ [8]

$$\mathbf{R}=\sum_{f_1,f_2} W(f_1,f_2)\left\{S_{\text{expt}}(f_1,f_2)-\sum_{\beta=0}^{\pi/2} P^*(\beta)S_{\text{theor}}(f_1,f_2|\beta)\right\}^2 \quad (5)$$

under the constraint $P^*(\beta)\geq 0$. $W(f_1,f_2)$ is a symmetric matrix which accounts for weighting of different parts of the spectrum according to signal to noise considerations. The position of the global minimum $P_{\min}(\beta)$ of $\mathbf{R}$ without constraint can be calculated analytically. $P_{\min}$ is then used to find a starting value for a steepest descent minimization of $\mathbf{R}$ to find the result with $P^*(\beta)\geq 0$ for all β.

C. Simulation of 2D exchange spectra for diffusion on a sphere

A random walk simulation of diffusion on a sphere as described previously [4] was used to simulate 2D exchange powder spectra. To check the minimization procedure (Sec. III B) and to investigate the influence of motions during the evolution time t_1 and the acquisition time t_2 on the resulting RAD $P^*(\beta)$, two types of simulations were performed: A simulation allowing random diffusion during t_1,t_2, and the mixing time t_m was compared with a simulation allowing diffusion only during t_m and assuming exponential relaxation during t_1 and t_2. In the latter case a relaxation time of $T_2=200$ μs was chosen.

In both cases 256 complex-time-domain data points were calculated for 128 t_1 values with dwell times of 5 μs in both dimensions. A quadrupolar splitting of 30 kHz was assumed and the simulation used 100 000 spins equally distributed over the sphere. The time-domain data were again analyzed in the same way as the experimental data to get the 2D simulation spectra. Diffusion simulations were carried out for three mixing times (2, 4, and 8 ms) and a diffusion correlation time τ_D of 4.267 ms, where $\tau_D=\tau_2$ as given by Eq. (2). This corresponds to a diffusion constant $D=4\times10^{-12}$ m^2/s and a radius of $R=320$ nm.

To calculate the RAD $P^*(\beta)$ of the different simulations, a set of 30 kernel functions was calculated and the minimization procedure as described above [Eq. (5)] was applied. During the simulation run the program simultaneously did a statistical analysis of the jumps occurring during the mixing time to check the random walk diffusion simulation. The result for a mixing time of 4 ms and a correlation time of 4.2667 ms is shown in Fig. 1. As can be seen from the solid theoretical curve the simulation represents very well a diffusional process on a sphere. The scatter in the statistics comes from noise in the simulation as only 100 000 spins were simulated.

IV. SIMULATION RESULTS

Figure 2 shows the 2D exchange spectra from simulations of diffusion on a sphere for a correlation time of

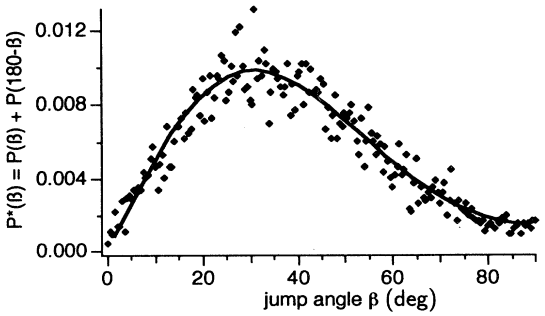

FIG. 1. Statistics of the jump angle β from the simulation program. The correlation time of the simulated diffusion process is 4.2667 ms and the mixing time 4 ms. The line shows the theoretical jump angle distribution $P^*(\beta)$ for the parameters (cf. Sec. III A). The scatter comes from statistical noise in the simulation, which was carried out with 100 000 diffusing spins.

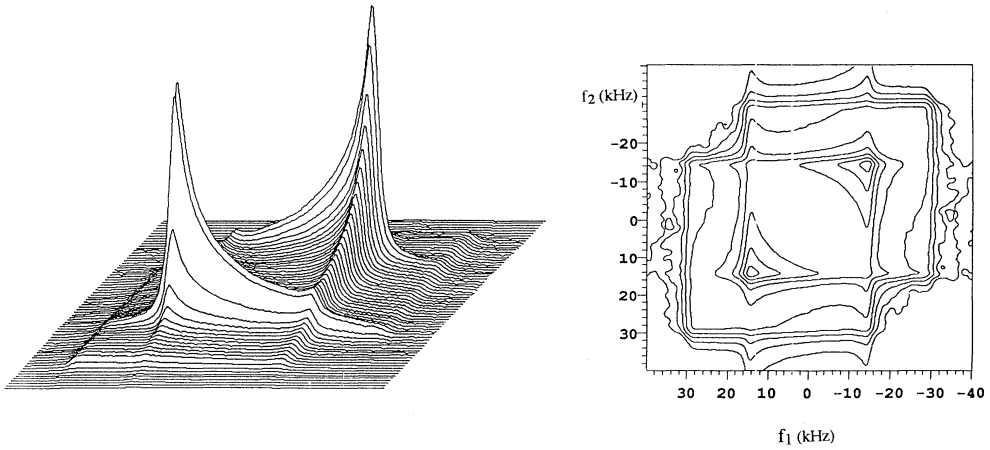

FIG. 2. Contour and stacked plots of 2D exchange spectrum from a diffusion simulation with a mixing time of 4 ms and a correlation time $\tau_D = 4.267$ ms. The frequency scales for f_1, the abscissa, and f_2, the ordinate, of the stacked plot are the same as those shown for the contour plot.

4.267 ms and a mixing time of 4 ms. Not shown are the spectra for $t_m = 2$ and 8 ms, which clearly show the sensitivity of the line shape to the ratio t_m/τ_D. As already pointed out in [5] and [22], the line shape shows a significant increase in the off-diagonal intensity at a ratio $t_m/\tau_D > 1$, thus giving a measure for the correlation time of the underlying motional process.

Figure 3 shows the jump angle distribution $P^*(\beta)$ calculated by the minimization procedure [see Eq. (5)] from simulations with a correlation time of 4.2667 ms. In the histogram of Fig. 3(a) the resulting $P^*(\beta)$ distributions for a mixing time of 4 ms of a simulation allowing no diffusion during t_1 and t_2 (cf. Sec. III C) can be seen. The solid line represents the theoretical prediction for $P^*(\beta)$ as described in Sec. III A for the corresponding mixing and correlation times. The jump angle distribution $P^*(\beta)$ from a simulation with the same correlation and mixing times but now allowing diffusion during all times, including during t_1 and t_2, is shown in Fig. 3(b) and compared with the same theoretical curve (solid line) as in Fig. 3(a).

For an estimate of the error in the correlation time τ_D, a set of theoretical jump angle distributions for different τ_D was used to calculate their squared deviation from the minimization procedure result. In the case of a simulation allowing no diffusion during t_1 and t_2, the minimum in the squared deviation yields a correlation time of 4.25 ± 0.2 ms for all mixing times (2, 7, and 8 ms). The second type of simulation, allowing diffusion at all times, gives thus a correlation time of 4.4 ± 0.4 ms ($t_m = 2$ ms), 4.4 ± 0.4 ms ($t_m = 4$ ms) and 4.25 ± 0.4 ms ($t_m = 8$ ms). We conclude that the approximation $t_1, t_2 \ll \tau_D$ is satisfied within the computational error in this case.

Not shown are results for a simulation with faster diffusion ($\tau_D = 1.667$ ms) and mixing times of 2 and 4 ms. In this case a simulation without diffusion during t_1 and t_2 yields a jump angle distribution $P^*(\beta)$ with a correlation time of 1.7 ± 0.15 ms for all mixing times. The second type of simulation gives correlation times of 1.4 ± 0.25 ms ($t_m = 2$ ms) and 1.6 ± 0.2 ms ($t_m = 4$ ms). In this case of a shorter τ_D, there is some indication that the effect of diffusion during t_1 and t_2 is manifesting itself in shifting the apparent correlation time towards shorter values. Even in this case, however, the results with and without the inclusion of diffusion t_1 and t_2 agree within the computational error.

V. EXPERIMENTAL RESULTS

2D exchange experiments were performed on two different types of samples. Figure 4 shows contour and stacked plots of spectra from a fully hydrated POPC-6-d_2 SSMV sample (20 wt % water) at a temperature of 30 °C. Mixing times were 2 ms [Fig. 4(a)] and 4 ms [Fig. 4(b)].

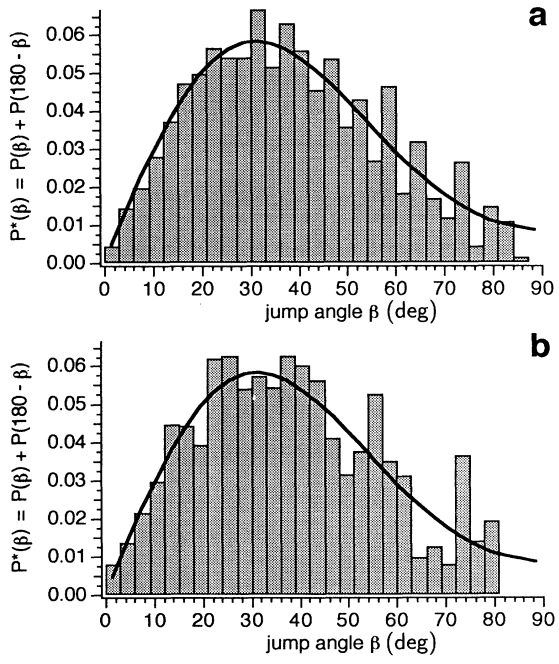

FIG. 3. Jump angle distribution (RAD) $P^*(\beta)$ from a diffusion simulation with a mixing time of 4 ms and a correlation time of 4.267 m. The simulation in (a) was carried out with no diffusion during t_1 and t_2 (cf. Sec. III C) while that in (b) allowed diffusion at all times, including during t_1 and t_2. The solid line in each case represents the theoretical prediction for $P^*(\beta)$ assuming diffusion on a sphere as described in Sec. III A, including the corresponding mixing and correlation times. $P^*(\beta)$ was calculated by the minimization procedure [Eq. (5)].

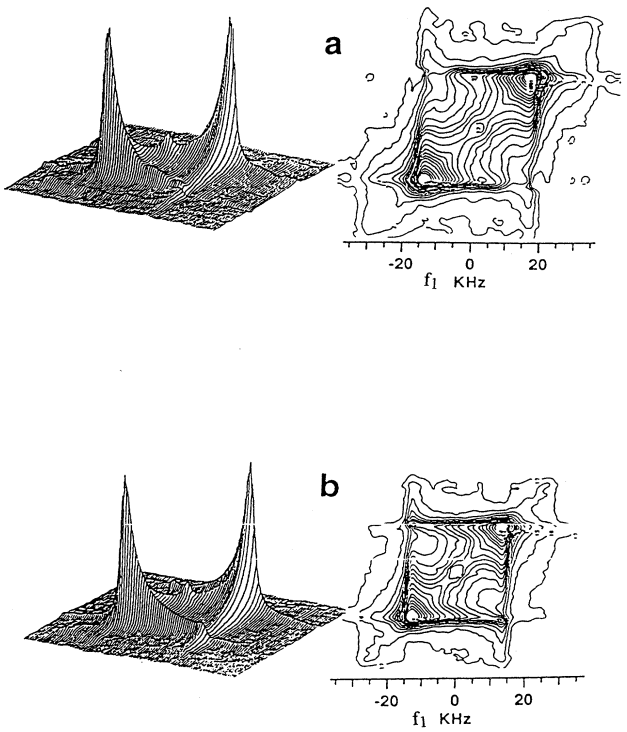

FIG. 4. Stacked plots and contour plots of experimental 2D exchange spectra of POPC-6-d_2 spherical supported multilamellar vesicles at full hydration at 30 °C with mixing times of 2 ms (a) and 4 ms (b). The scale for the ordinate f_2 is the same as for the abscissa f_1.

The spectrum of the low hydration sample (7 wt % H_2O, cf. Sec. II), recorded at a temperature of 35 °C and with a mixing time of 4 ms, is shown in Fig. 5.

In comparing the diagonal intensities one can see that in the low hydration sample the quadrupolar splitting (38.4 kHz) is higher than in the fully hydrated sample (30.2 kHz). The off-diagonal intensity of the low hydration 2D spectrum at $t_m = 4$ ms is remarkably lower than in the fully hydrated sample at the same mixing time, showing a much longer correlation time of the underlying motion in the first case.

This is demonstrated quantitatively by the jump angle distribution $P^*(\beta)$ calculated by the minimization procedure (cf. Sec. II B). The bar diagrams in Fig. 6 show the experimental results for $P^*(\beta)$ from the fully hydrated sample. The solid line represents the best fit of the theoretical jump angle distribution for isotropic lateral diffusion on the surface of a sphere with a correlation time τ_D [cf. τ_2 in Eq. (3)]. The experimental $P^*(\beta)$ can be fitted best by the theoretical prediction for $P^*(\beta)$ (cf. Sec. III A) assuming one single motional correlation time of $\tau_D = 2.7 \pm 0.5$ ms for $t_m = 2$ ms and $\tau_D = 3.0 \pm 0.5$ ms for $t_m = 4$ ms. The error in τ_D was estimated by a least squares fit of a set of theoretical $P^*(\beta)$ curves to the experimental $P^*(\beta)$ from the minimization procedure.

In the low hydration case, the minimization procedure gives a $P^*(\beta)$ which can be best fitted by a theoretical $P^*(\beta)$ assuming a diffusion correlation time of 32 ± 10 ms. In this case the error in τ_D is bigger because $t_m/\tau_D = 0.1$. At this ratio t_m/τ_D, the shape variation of the jump angle distribution $P^*(\beta)$ with the correlation time is unfortunately small and thus the accuracy in the determination of τ_D is reduced.

VI. DISCUSSION

A. Lipid lateral diffusion

There are at least three independent contributions to the off-diagonal elements of $S(\omega_1, \omega_2, t_m)$. These are (1) lateral diffusion of the phospholipids along a curved bilayer surface, (2) thermally excited collective surface undulations of the bilayer, and (3) collective director fluctuations. For further application of the method to more complex systems it is of great importance to separate the different contributions. In contrast to discrete jump motions, where characteristic ridges (e.g., ellipsoids) are observed in the spectrum, all of the above mentioned mechanisms give more complex patterns which may prevent a straightforward analysis in terms of a jump angle distribution function. Our work concentrates on the effect of lateral diffusion. We use a spherical membrane model system which has been established as geometrically well defined and for which lateral diffusion has been shown to be the dominant transverse relaxation mechanism [16].

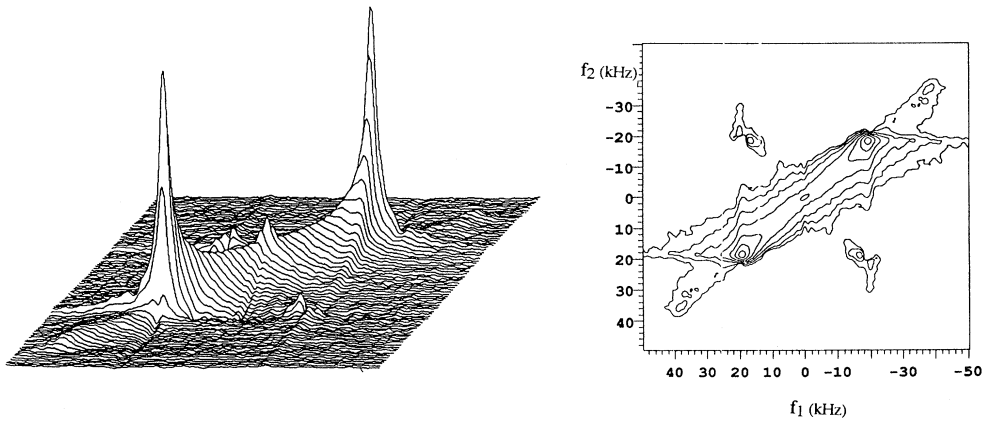

FIG. 5. Contour plot and stacked plot of experimental 2D exchange spectrum of POPC-6-d_2 SSMV at low hydration at 35 °C with a mixing time of 4 ms. The scales for the abscissa f_1 and the ordinate f_2 for the stacked plot are the same as those shown for the contour plot.

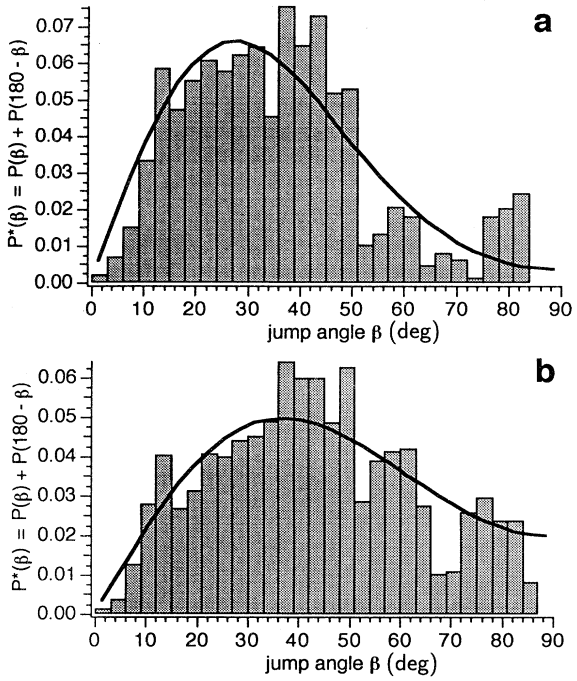

FIG. 6. Experimental jump angle distributions $P^*(\beta)$ of POPC-6-d_2 SSMV at full hydration (20 wt %) for mixing times of 2 ms (a) and 4 ms (b). Also shown is the best fit of a theoretical $P^*(\beta)$ curve (cf. Sec. III) to the experimental result for the corresponding mixing times. This gives a correlation time τ_D for diffusion on a sphere of $\tau_D = 2.75$ ms (a) and 3.0 ms (b).

The phase acquisition of spins diffusing freely on the surface of a sphere during an echo experiment can be simulated by a random walk jump diffusion process for a given diffusion coefficient D and sphere radius R [23]. This enables us to check the reliability of our approach to the calculation of $P^*(\beta)$ in terms of lateral diffusion as the sole slow motion mechanism by analyzing the simulation time-domain data in exactly the same way as was done for the experimental ones. As shown in Fig. 3, good agreement is obtained between the simulated and theoretical $P^*(\beta)$ for identical values of τ_D. The power of the simulation becomes even more obvious by considering the effect of diffusion during the preparation and detection period. It is usually assumed in the analysis of 2D spectra that the effect of the slow motion during the preparation and detection is negligible. In our experiments, we estimate $\tau_D \approx 4$ ms, while the largest values of t_1 and t_2 used to define the spectra are 0.6 ms. Thus it is not obvious *a priori* that the influence of diffusion during the preparation and detection period can really be neglected. However, the simulation results provide justification for neglecting the diffusion contribution during preparation and detection in treating our experimental data. They demonstrate that correlations to $P^*(\beta)$ due to diffusion during these periods are well within the experimental uncertainties under the conditions of our experiments.

It is now interesting to compare the simulated data with the those obtained experimentally for selectively deuterated POPC-6-d_2 which exhibits a quadrupolar splitting corresponding to that used in the simulations. The comparison can be made because the diameter of the spherical solid support of the experimental model system is known. A comparison of simulated and experimental spectra for $t_m = 4$ ms (cf. Figs. 2 and 4) does not show any significant differences, in both cases a similar amount of off-diagonal intensity is present. A more detailed comparison is obtained by looking at the $P^*(\beta)$ jump angle distributions for both cases: It is not clear whether the higher probabilities at jump angles $\beta > 75°$ for the experimental data relative to the theoretical predictions are statistically significant. Such an overestimate was also obtained in the simulation experiment (Fig. 3) and might be due to the effect of the diffusion during the preparation and detection periods.

The value of $\tau_D = 3 \pm 0.5$ ms obtained as the best fit from the minimization procedure of the experimental data for $t_m = 4$ ms and $T = 30\,°C$ is less than the one used for the simulation, where $D = 4 \times 10^{-12}$ m^2/s ($\tau_D = 4.26$ ms) was used. This value of D was previously measured by us for a single POPC bilayer on a spherical support of the same diameter ($R = 320$ nm) at 30 °C using transverse ^{2}H NMR relaxation [16]. The discrepancy indicates that the diffusion coefficient D is higher for the supported POPC multilayer system used in the present work than measured for the single bilayer. For calculating D from τ_D we have to use a radius R of the system which is larger than that of the spherical support since we have an average of 20 bilayers coated to the beads. Using a bilayer repeat distance of 60 Å [24] and considering the radius error of the beads (± 20 nm), we end up with an average radius of $\langle R \rangle = 290 \pm 60$) nm. Using this average radius and $\tau_D = 3.0$ ms we obtain a diffusion coefficient of $D = (8.2 \pm 3) \times 10^{-12}$ m^2/s. This value is in good agreement with $D = (5 \pm 0.6) \times 10^{-12}$ m^2/s as obtained by the fluorescence recovery after photobleaching (FRAP) technique for fully hydrated POPC multilayers at 30 °C [25] and matches equally well with $D = (6.0 \pm 2) \times 10^{-12}$ m^2/s measured at 35 °C for POPC multilayers using the pulsed field gradient (PFG) NMR technique [26].

It should be emphasized that the characteristic length scale of the 2D exchange ^{2}H NMR experiment is similar to that for PFG measurements (≤ 1 μm) while the FRAP method averages over an order of magnitude larger length scale. In contrast, the above mentioned transverse relaxation method which gave the lower D value used for our simulations ($D = 4 \times 10^{-12}$ m^2/s) has a length scale of less than 100 nm. This distinction might account in part for the differences in D. Another origin for the lower D in the case of the single bilayer could be friction between the bilayer and the surface of the solid support [25].

In general, the good agreement of the diffusion constant D extracted form the 2D exchange experiment with FRAP and PFG measurements indicates the following. (1) Lateral diffusion of the lipids along the spherical bilayer is the only relevant mechanism which contributes to $S(\omega_1, \omega_2, t_m)$ for the case of lipid bilayers on a spherical support. (2) The basic assumptions made in our analysis of the experimental data are still correct; in particular,

neither local bilayer thickness nor curvature fluctuations occur in our model system to an extent that they can contribute to $S(\omega_1,\omega_2;t_m)$.

Thus we have a situation which differs markedly from that encountered in the accompanying paper [14] where multilamellar vesicles without support were studied. For multilamellar vesicles there are contributions to $S(\omega_1,\omega_2,t_m)$ which cannot be explained by lateral diffusion of lipids on spherical surfaces. This demonstrates the potential of the method to tackle the elusive problem of identifying other fluctuation processes on the mesoscopic length scale in bilayers. This can be achieved by isolating contributions such as lateral diffusion by comparative measurements using geometrically defined model systems.

B. The effect of hydration

Comparing the off-diagonal intensities of the low hydrated sample (7 wt % H_2O) (Fig. 5) obtained at a mixing time $t_m=4$ ms with the fully hydrated samples (20 wt %) at $t_m=2$ ms [Fig. 4(a)], one can estimate that the correlation time in the first case is at least a factor of 2 bigger than in the fully hydrated sample. This indicates a significant drop of the lateral diffusion coefficient D due to the lower hydration. In fact, a reduction in D by a factor of 2.5 between the fully hydrated (40 wt % D_2O) and the low hydrated (15 wt % D_2O) state for multilayer of the saturated phospholipid DPPC is well known from the literature [27]. Using quasielastic neutron scattering, a reduction of D for the same lipid by a factor of 4.1 was observed between 23 and 8 wt % hydration [28]. The minimization procedure for our data obtained at $t_m=4$ ms and at 7 wt % H_2O gives a value of $\tau_D=32\pm10$ ms for the diffusion correlation time and thus $D=(0.8\pm0.4)\times10^{-12}$ m^2/s, using the same assumptions as in Sec. VI A.

C. Effect of transverse relaxation during mixing and detection periods

As stated above, one of the useful results of the simulation studies was the demonstration that, although diffusion during the evolution and detection periods has a measurable effect on the 2D NMR exchange spectrum, its neglect in the analysis does not result in large errors in $P^*(\beta)$ for the values of τ_D and S_{CD} that apply to the system studied. This would no longer be true for a system characterized by appreciably shorter values of τ_D as we have found and was predicted in earlier work by Kaufmann *et al.* [29]. No simple procedure is available presently for taking into account the influence of diffusion during the regions before and after the mixing region.

One approximate method of handling this problem would be to include a correction in the form of the type of orientation-dependent transverse relaxation that is known to be caused by diffusion on curved surface [4]. In our analysis, we have corrected for transverse relaxation in a crude, *ad hoc* manner by multiplying the time-domain signal by $\exp[-(t_1+t_2)/T_2)]$ while assuming that T_2 is constant independent of frequency.

In practice we know that the random phase arising from diffusion on a sphere gives rise to more complex, nonexponential relaxation of the quadrupolar echo amplitude $S(2\tau)$ [4,30]. At short times the leading term in $S(2\tau)$ is given by

$$S(2\tau)\approx S(0)\exp[-6(\omega_q S_{CD})^2(\tau_D)^{-1}\sin^2\theta\cos^2\theta\tau^3]\ . \quad (6)$$

The dependence on θ results in a strong dependence of the transverse relaxation on spectral frequency. It is likely that a correction factor based on such a frequency-dependent transverse relaxation behavior will at least partially compensate for the influence of diffusion during evolution and detection regions and we plan to discuss this in a forthcoming paper.

VII. CONCLUSION

We have shown that 2D exchange NMR spectra obtained on spherical supported lipid bilayers can be satisfactorily explained on the basis of lateral diffusion of lipids on a spherical surface. In the accompanying paper [14], a similar study of a dispersion of unconstrained multilamellar vesicles showed that at short mixing times a large fraction of the lipids behaved as though they were diffusing on highly curved surfaces. At longer mixing times, most of these lipids exhibited a behavior characteristic of much larger radii of curvature. Such observations are consistent with diffusion on a rough surface having a relatively large average radius of curvature. The fact that the data presented in this paper do not exhibit effects of surface roughness, when combined with the results for the unconstrained multilamellar vesicles, indicates the potential of the method for future applications in the field of membranes in providing geometrical information about the objects under study together with the time correlation function. This can be achieved by comparing measurements on complicated systems with those on the type of simple model systems studied in this work.

[1] M. Bloom and E. Sternin, Biochemistry **26**, 2101 (1987).
[2] P. I. Watnick, P. Dea, and S. Chan, Proc. Natl. Acad. Sci. U. S. A. **87**, 2082 (1990).
[3] J. Stohrer, G. Gröbner, D. Reimer, K. Weisz, C. Mayer, and G. Kothe, J. Chem. Phys. **95**, 672 (1991).
[4] C. Dolainsky, A. Möps, and T. M. Bayerl, J. Chem. Phys. **98**, 1712 (1993).
[5] C. Schmidt, B. Blümich, and H. W. Spiess, J. Magn. Reson. **79**, 269 (1988).
[6] S. Wefing and H. W. Spiess, J. Chem. Phys. **89**, 1219 (1988).
[7] S. Wefing, S. Kaufmann, and H. W. Spiess, J. Chem. Phys. **89**, 1234 (1988).
[8] H. Hagemeyer, L. Brombacher, K. Schmidt-Rohr, and H. W. Spiess, Chem. Phys. Lett. **167**, 583 (1990).
[9] M. Auger and H. C. Jarrell, Chem. Phys. Lett. **165**, 162 (1990).
[10] M. Auger, I. P. Smith, and H. C. Jarrell, Biophys. J. **59**, 31

(1991).
[11] D. B. Fenske and H. C. Jarrell, Biophys. J. **59**, 55 (1991).
[12] D. B. Fenske and P. R. Cullis, Biochim. Biophys. Acta **1108**, 201 (1992).
[13] J. H. Ipsen, O. G. Mouritsen, and M. Bloom, Biophys. J. **57**, 405 (1990).
[14] F. Macquaire and M. Bloom, preceding paper, Phys. Rev. E **51**, 4735 (1995).
[15] T. M. Bayerl and M. Bloom, Biophys. J **58**, 357 (1990).
[16] T. Köchy and T. M. Bayerl, Phys. Rev. E **47**, 2109 (1993).
[17] E. Sternin, Rev. Sci. Instrum. **56**, 2043 (1985).
[18] D. I. Hoult and R. E. Richards, Proc. R Soc. London **344**, 311 (1975).
[19] Y. K. Levine and A. I. Bailey, Nature **220**, 557 (1968).
[20] L. Greenspan, J. Res. Natl. Bur. Stand. Sect. A **81A**, 89 (1977).
[21] D. Grabowski and J. Hohnerkamp, J. Chem. Phys. **96**, 2629 (1992).
[22] B. D. Fenske, M. Letellier, R. Roy, I. C. P. Smith, and H. C. Jarrell, Biochemistry **30**, 10 524 (1991).
[23] C. Dolainsky, T. Köchy, C. Naumann, T. Brumm, S. J. Johnson, and T. M. Bayerl, in *The Structure and Conformation of Amphiphilic Membranes,* edited by R. Lipowski, D. Richter, and K. Kremer (Springer-Verlag, Berlin, 1992), p. 34.
[24] J. F. Nagle and M. C. Wiener, Biochim. Biophys. Acta **942**, 1 (1988).
[25] R. Merkel, E. Sackmann, and E. Evans, J. Phys. (Paris) **50**, 1535 (1989).
[26] G. Lindblom, L. B.-A. Johansson, and G. Arvidson, Biochemistry **20**, 2204 (1981).
[27] A.-L. Kuo and C. G. Wade, Biochemistry **18**, 2300 (1979).
[28] S. König, W. Pfeiffer, T. Bayerl, D. Richter, and E. Sackmann, J. Phys. II (France) **2**, 1589 (1992).
[29] S. Kaufmann, S. Wefing, D. Schaefer, and H. W. Spiess, J. Chem. Phys. **93**, 197 (1990).
[30] M. Bloom, C. Morrison, E. Sternin, and J. L. Thewalt, in *Pulsed Magnetic Resonance: NMR, ESR and Optics, a Recognition of E. L. Hahn,* edited by D. M. S. Bagguley (Clarendon, Oxford, 1992), p. 274.